



# Journal of Applied Sciences

ISSN 1812-5654

**science**  
alert

**ANSI***net*  
an open access publisher  
<http://ansinet.com>

## Investigation of Microstructure and Mechanical Behavior of AlSi7 Mg

<sup>1</sup>V. Sankar and <sup>2</sup>S. Muthu

<sup>1</sup>Anna University, Chennai, Tamil Nadu, India

<sup>2</sup>Dr. N.G.P. Institute of Technology, Coimbatore, Tamil Nadu, India

**Abstract:** Heat treatment of A356 alloys in combined addition of rare earth and strontium was conducted. T6 treatment is a long time treatment (solution at 525°C for 8 h+aging at 165°C for 8 h). The effects of heat treatment on microstructure and tensile properties of the Al-7Si-0.3 Mg alloys were investigated by optical microscopy METSCOPE-1, scanning electronic microscopy and tension test. It is found that an 8 h solution at 525°C is sufficient to make homogenization and saturation of magnesium and silicon in 8 (Al) phase, a spheroid of eutectic Si phase. Followed by solution, an 8 h artificial aging at 165°C is almost enough to produce hardening precipitates. Those samples treated with T6 achieve the maximum tensile strength 324 Mpa, yield stress 228 MPa and fracture elongation 2.0%.

**Key words:** Al-Si casting alloys, heat treatment, tensile stress, microstructure analysis

### INTRODUCTION

The aging-hardenable cast aluminum alloys, such as A356, are being increasingly used in the railway and aerospace industries due to their relatively high specific strength and low cost, providing affordable improvements in fuel efficiency. The autistic structure of A 316 can be refined and its properties can be improved by optimized heat treatment for A356 and A 316 under without treating process. T6 heat treatment is usually used to improve fracture toughness and yield strength. It is reported that those factors influencing the efficiency of heat treatment of Al-Si hypoeutectic alloys include not only the temperature and holding time, (Edwards *et al.*, 1998; Ran *et al.*, 2008) but also the as-cast microstructure. Zolotarevsky *et al.* (2007), Li *et al.* (2007) and Shi *et al.* (2010). The T6 heat treatment of Al-7Si-0.3 Mg alloy includes two steps: Solution and artificial aging; the solution step is to achieve 8 (Al) saturated with Si and Mg and spheroidized Si in eutectic zone (Yu *et al.*, 2009; Ran *et al.*, 2008; Lee *et al.*, 2008). While the artificial aging is to achieve strengthening phase Mg<sub>2</sub>Si. Recently, it is shown that the spheroidization time of Si is dependent on solution temperature and the original Si particle size. Gao *et al.* (2008), Xiao *et al.* (2003), Gao *et al.* (2007) and Lee *et al.* (2004) A solution treatment time of 8 h. From thermal diffusion calculation and test, it is suggested that the optimum solution soaking time at 525°C is 8 h. The maximum peak aging time was modeled in terms of aging temperature and activation energy. According to this model, the peak yield strength of A356 alloy could be reached within 3-8 h when aging at 165°C (Yang, 2003;

Liu and Xue, 2006; Zhang *et al.*, 2002). However, few studies are on the effect of combined treatment with solution and aging. In this study, using this alloy modified together with Si and Al, the effect of different heat treatments on the microstructure and its mechanical properties were investigated.

### EXPERIMENTAL PROCEDURE

Commercially pure aluminum and silicon were melted in crucible furnaces. AlSi7 Mg master alloy modified using Al-6.728 Si and Al-91.26 RE master alloy use the alloy refined. The chemical composition of this A356 alloy ingot (Table 1) was checked by utilizing spectrometer. Before the casting, the hydrogen contents of about 0.25 cm by 100 gm in the metal was measured by ELH-III. Four bars of 50×70×120 mm were produced by the same ingot by machine and were heat-treated according to the (Table 2) followed the solution, bars were quenched in the oil medium of 525°C. Tests cut from the cast ingot and heat-treated bars were polished reason and corroded used HF agent of 0.5%. Optical microscope METSCOPE-1 and the scanning of electric microscope UTM-FIE was used to examine the microstructure and fractograph. To measure the eutectic Si morphology change of different heat treatments an image analyzer Mic 2.0 was used and every measurement enclosed 800-1200 particles. Tensile patterns were produced from the modified bars. The tensile tests were carried out, a FIE using, do universal tensile testing machine (UTE-100) in the air with ambient temperature. The applied strength was 88300 N. The strain was measured, extensometer enclosed of the test and with a

Table 1: Chemical composition of A356 modified with Ti, Si and RE (mass fraction %)

Si	Fe	Sn	Cu	Mn	Mg	Zn	Cr	Ni	Ti	Al (Reminder)
6.728	0.378	0.250	0.185	0.064	0.223	0.165	0.009	0.161	0.036	91.26

Table 2: Quenched solution bass in the oil of 525°C

Solution			Aging	
Treatment	Temperature (°C)	Holding time (h)	Temperature (°C)	Holding time (h)
T6	525 ± 5	8	165	8

measuring length of 52 mm. The 152 MPa proof stresses were used as the yield stress of alloy. Multiple tests were checked for every heat treatment to calculate the average.

Tensile patterns were produced from the modified bars. The tensile tests were carried out, a FIE using, do universal tensile testing machine (UTE-100) in the air with ambient temperature. The applied strength was 88300 N. The strain was measured, extensometer enclosed of the test and with a measuring length of 52 mm. The 152 MPa proof stresses were used as the yield stress of alloy. Multiple tests were checked for every heat treatment to calculate the average.

## RESULTS AND DISCUSSION

**Microstructure characterization of as-cast alloy:** The microstructure of the cast A356 alloy is shown in Fig. 1a. It is shown that not only the prefix 8 (Al) becomes a dendrite cell refined, but also the eutectic silicon is well modified. By means of the image analysis, microstructure-frame of the cast A356 alloy were analyzed statistically as follows: 8 (Al) is a dendrite -cell size 76.1 μm silicone particle-size is 2.2×1.03 μm (length×width) and the ratio aspect of silicone is 2.13. The distribution of RE (mish rare metal earth, La of more than 65% among them), Ti, mg and Sr in the area shown in Fig. 1b is presented in Fig. 1c-f. It is shown that the eutectic silicone particle is normally covered with Sr which plays a key role in the Si particle modification; Ti and RE present generally uniform distribution about the observed area, although a slight separation is observed by RE and is shown in Fig. 1d. It is suggested, that because the refiner Ti2Al3 and TiB are covered with RE which is improved refining efficiency significantly. In the alloy of the cast some cluster of mg probably indicate that coarser Mg2Si phases as shown in Fig. 1d. Ti solute can limit the growth from 8 (Al) primary dendrite because of its high growth restriction factor (17). The impediment of formation of poisoning Ti Si composition around TiAl3 and doctorate of Ti (Al1-X Six) 3 films covering the TiB2 is very important in the Al-Si- alloy refining. Because Al-Si interferes with, the effect from RE on the refining

efficiency of Ti and B can be contributed to the following causes: preventing refiner phases from poisoning; retarding the TiB2 phase to a mass accumulate and to sink; the Ti (Al, Si) 3 compound growth supporting to cover the TiB2 phase. In this work, with the suitable addition of Re and Sr, the microstructure of the A356 alloy was optimized. Especially eutectic Si is completely modified who is advantageous to promote Si spheroidize further during the solution treatment.

**Microstructure evolution during heat treatment:** The microstructures of A356 alloy treated with solution in 550°C for 8 h and solution treatment, as shown in Fig. 2(a-b), while those which are treated with solution in 535°C for 8 h and T6 treatment as shown in Fig. 2(c-d), From Fig. 1 and 2, after heat treatments, the prefix 8 (Al) has somewhat been and the eutectic silicon has been next spheroidized. Both solution treatment and as well as Solution heat treated and then artificially aged treatments generate almost the same microstructure. The eutectic Si particle distribution and statistical mean aspect ratios of the eutectic Si particle are shown in Fig. 3. Afterwards only solution in 535°C for 8 h the middle picture sides formats of the Si are 1.57 and 1.54, respectively.

Treated by the ST and T6, those aspect ratios Si do not change exceptionally and they are 1.49 and 1.48, respectively. After the solution or solution which becomes aging in this study is the friction of eutectic Si particles with aspect ratio of 1.5 is 50%. The eutectic which melts attack temperature of Al7Si mg was more than 560°C. 550°C are under the liquid steady phase zone. During the solution two steps come at the same time, i.e., the formation of the solution of Al saturated with the Si and mg and spheroidization of the fibrous Si particle. The following model forecasts that decay and spheroidization are finished by eutectic silicone corals in 540°C after a few minutes (τ max).

Where  $\phi$  the atomic diameter of silicone;  $\gamma$  the Al/Si- symbolizes the interfacial energy;  $r_0$  is the original radius of the fibrous Si; D the inter-diffusion coefficient of the Si in Al and T is the solution temperature. If the Ds variation at different temperatures, it is to be suggested

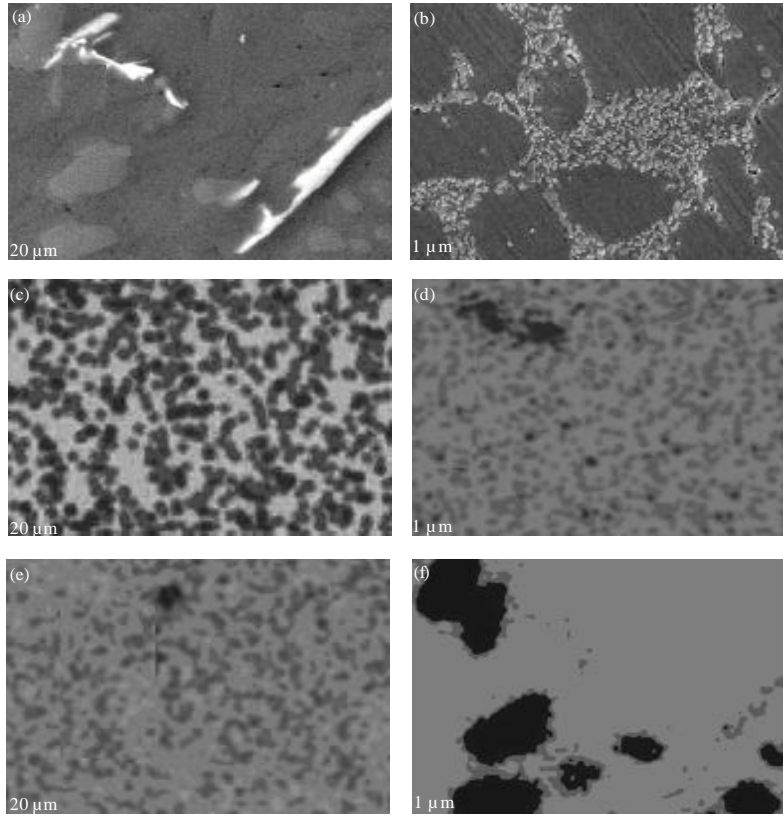


Fig. 1(a-f): (a, b) SEM images, (b) EDS mapping for (c) 0.038% Ti, (d) 65% La, (e) 0.106% Mg and (f) Sr in as-cast alloy

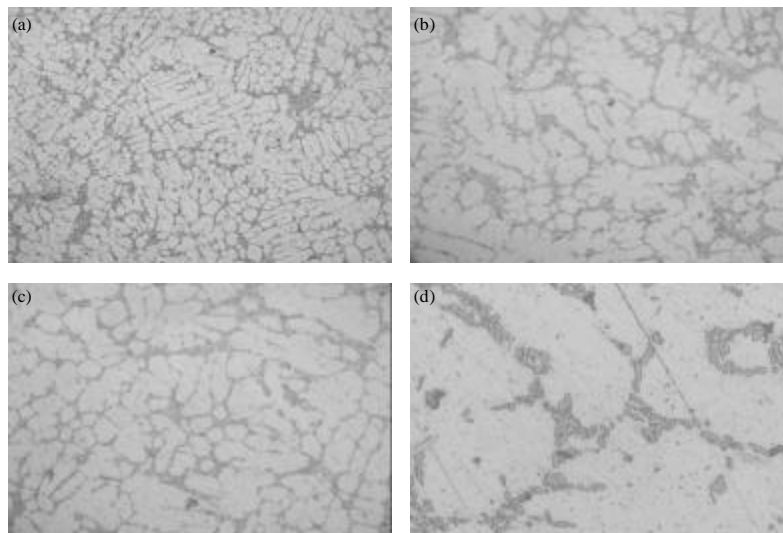


Fig. 2(a-d): Microstructure of A356 alloy with different heat treatments solution at 525°C for 8 h; T6 treatment (The microstructure shows Al-Si particles in a matrix of aluminium solid solution. Eutectic particles are fine globular and some are agglomerated in the matrix)

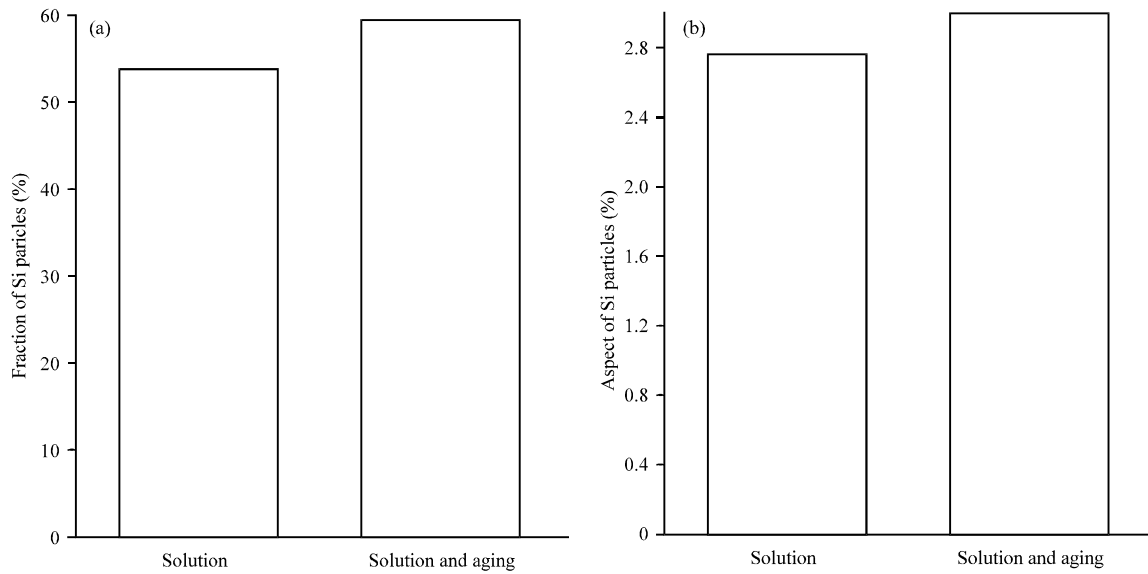


Fig. 3(a-b): Heat treatment of solution and then artificially aged (T6) (a) Solution, solution and aging vs. fraction of Si particle and (b) Solution, solution and aging vs. aspect ratio of Si particle

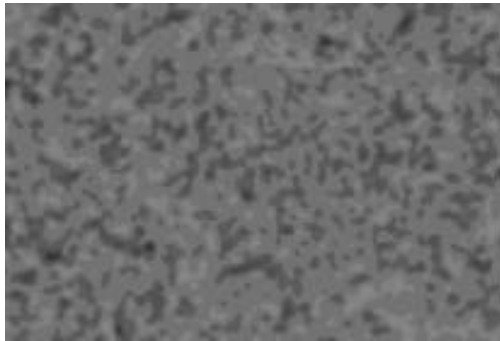


Fig. 4: SEM image of Mg distribution in alloy after only solution at 525°C for 8 h

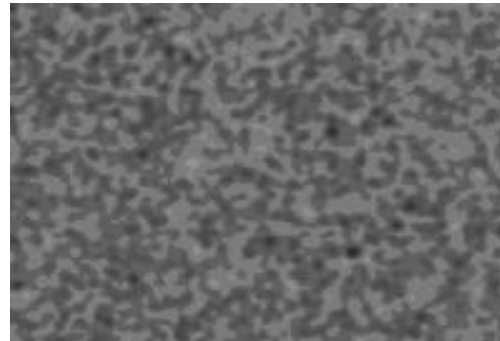


Fig. 5: SEM image in alloy after modification of solution with heat and then artificially aged

plausible that the distribution of Mg is uniform in the dendrite cell zone of Al and eutectic zone as shown in Fig. 4 and 5.

According to the study by ROMETSCH and SCHAFFER (14) is the time to reach maximum yield, 2-4 h and 12 - 14 h in 170°C and 150°C respectively. From 150 to 190°C of the aging temperature the maximum hardness changes between HB110 and HB120. Consequently it is believed of the fact that aging generates almost the same precipitation in 170°C for 8 h which hardens like, in 150°C for 15 h as aging.

**Tensile properties of A356 alloys:** The tensile qualities of A356 alloy are given in the Table 3. Because of the

Heat treatment	$\sigma_b$ /Mpa	$\sigma_t$ /Mpa	$\delta$ (%)
T6	228	324	2.0

microstructure-optimization of the A356 alloy by means of the combination of the refining and modification about 210 MPa and 3.7% or can reach train load and elongation. Using T6 treatment in this study, strength and elongation can be improved significantly. For those tests with the T6 treatment the train load and elasticity present the maximum values. The 90% of the maximum profit strength, 95% of the maximum extreme strength and 80% of the maximum elongation can be reached for tests treated by the ST. treatment. However, T6 treatment spends about

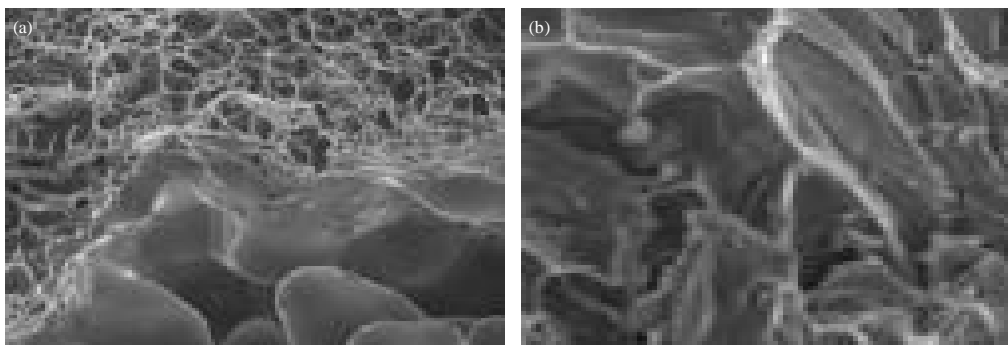


Fig. 6(a-b): Fractographs of samples heat treatment

8 h, while ST. Treatment takes only about 4 h. Fractographs of tests negotiated with T6 are presented in Fig. 6.

$$\tau_{\max} = \frac{32\pi^2}{9} \cdot \frac{kT}{D_s \gamma} \cdot \left( \frac{\rho}{\phi} \right) \ln \frac{\rho}{\phi}$$

The dimple size is similar almost with different heat treatments, indicating that the size and spacing of the eutectic silicon particle change a little with different heat treatments. Shrinkage pore, micro-crack within the silicon particle and crack linkage between eutectic silicon particles was observed on the break surfaces.

One knows far away that shrinkage pores have a big effect on the tensile and elasticity of A356 alloy. In-situ SEM fracture of the A356 alloy indicates the break result as follows (4): Micro-crack introduction within the silicon particle; formation of the slipping band in the dendrite of Al; linkage between the macro-crack and micro-crack and the growth of the crack. During the tensile strain inhomogeneous deformation in the microstructure arrange internal stresses in the eutectic silicon and Fe bearing intermetallic particles. Although the full modification of the eutectic Si particle was reached in this study, those tests with T6 treatment negotiated do not perform as well as expected. The principal reason is likely because of the higher gas contents (0.25 cm<sup>3</sup> per 100 g Al). Our following step is to develop new means, to purify the AlSi alloy to improve their mechanical qualities. Our following step is to develop new means, to purify the AlSi alloys to improve their mechanical qualities next.

### CONCLUSION

The solution in 535°C for 8 h full spheroidization of the Si particle, about the saturation of the Si and Mg reach. After T6 as well as ST treatments, the aspect ratio of the eutectic Si particle of 2.13 to less than 1.6 is reduced

and the friction of eutectic Si particles with the aspect ratio of 1.5 is 50%. The T6 treatment the maximum strength and the fracture elongation for A356 alloy is given by 324 MPa, yield stress 228 MPa. The T6 treatment can make the maximum strength and 80% of the maximum elongation 2.0% can be reached.

### REFERENCES

- Edwards, G.A., K. Stiller, G.L. Dunlop and M.J. Couper, 1998. The precipitation sequence in Al-Mg-Si alloys. *Acta Mater.*, 46: 3893-3904.
- Gao, B., L. Chen, S. Sun, G. Tu and X. Tian *et al.*, 2007. Effect of Nd on microstructure and mechanical properties of hypereutectic Al-25Si alloy. *J. Rare Earths*, 25: 473-476.
- Gao, Z.G., X.M. Zhang and M.A. Chen, 2008. Influence of strain rate on the precipitate microstructure in impacted aluminum alloy. *Scripta Materialia*, 59: 983-986.
- Lee, P.D., A. Chirazi, R.C. Atwood and W. Wang, 2004. Multiscale modelling of solidification microstructures, including microsegregation and microporosity, in an Al-Si-Cu alloy. *Mater. Sci. Eng. A*, 365: 57-65.
- Lee, K., Y.N. Kwon and S. Lee, 2008. Effects of eutectic silicon particles on tensile properties and fracture toughness of A356 aluminum alloys fabricated by low-pressure-casting, casting-forging and squeeze-casting processes. *J. Alloys Compounds*, 461: 532-541.
- Li, H.Z., X.P. Liang, F.F. Li, F.F. Guo, Z. Li and X.M. Zhang, 2007. Effect of Y content on microstructure and mechanical properties of 2519 aluminum alloy. *Trans. Nonferrous Metals Soc. China*, 17: 1194-1198.

- Liu, B.Y. and Y.J. Xue, 2006. Morphology transformation of eutectic Si in Al-Si alloy during solid solution treatment. *Special Casting Nonferrous Alloys*, 26: 802-802.
- Ran, G., J.E. Zhou and Q.G. Wang, 2008. Precipitates and tensile fracture mechanism in a sand cast A356 aluminum alloy. *J. Mater. Process. Technol.*, 207: 46-52.
- Shi, W.X., B. Gao, G.F. Tu and S.W. Li, 2010. Effect of Nd on microstructure and wear resistance of hypereutectic Al-20%Si alloy. *J. Alloys Compd.*, 508: 480-485.
- Xiao, D.H., J.N. Wang, D. Y. Ding and H.L. Yang, 2003. Effect of rare earth Ce addition on the microstructure and mechanical properties of an Al-Cu-Mg-Ag alloy. *J. Alloys Compounds*, 352: 84-88.
- Yang, L.J., 2003. The effect of casting temperature on the properties of squeeze cast aluminium and zinc alloys. *J. Mater. Process. Technol.*, 140: 391-396.
- Yu, Z.T., H.H. Zhang, B.L. Sun and G.J. Shao, 2009. Optimization of soaking time for T6 treatment of aluminium alloy. *Heat Treatment*, 24: 17-20.
- Zhang, D.L., L.H. Zheng and D.H. StJohn, 2002. Effect of a short solution treatment time on microstructure and mechanical properties of modified Al-7wt.% Si-0.3 wt.% Mg alloy. *J. Light Metals*, 2: 27-36.
- Zolotarevsky, V.S., N.A. Belov and M.V. Glazoff, 2007. *Casting Aluminum Alloys*. 1st Edn., Elsevier, Oxford, UK.